

Functional microbiome reprogramming links dietary interventions to neuroinflammatory outcomes in multiple sclerosis

Friederike Gutmann

friederike.gutmann@mdc-berlin.de

Max Delbrück Center for Molecular Medicine in the Helmholtz Association

Lina Samira Bahr

Max Delbrück Center for Molecular Medicine in the Helmholtz Association

Ulrike Brüning

Berlin Institute of Health (BIH) at Charité, BIH Metabolomics Platform

Víctor Hugo Jarquín-Díaz

Max Delbrück Center for Molecular Medicine in the Helmholtz Association

Lajos Markó

Max Delbrück Center for Molecular Medicine in the Helmholtz Association

Martin Weygandt

Charité – Universitätsmedizin Berlin, corporate member of Freie Universität Berlin and Humboldt-Universität zu Berlin

Rebekka Rust

Institute for Immunology at Charité Berlin

Judith Bellmann-Strobl

Max Delbrück Center for Molecular Medicine in the Helmholtz Association

Friedemann Paul

Max Delbrück Center for Molecular Medicine in the Helmholtz Association

Sofia K. Forslund-Startceva

Charité – Universitätsmedizin Berlin, corporate member of Freie Universität Berlin and Humboldt-Universität zu Berlin

Jennifer A. Kirwan

Berlin Institute of Health (BIH) at Charité, BIH Metabolomics Platform

Article

Keywords:

Posted Date: September 12th, 2025

DOI: https://doi.org/10.21203/rs.3.rs-7434844/v1

License: © (1) This work is licensed under a Creative Commons Attribution 4.0 International License.

Read Full License

Additional Declarations: No competing interests reported.

Abstract

Multiple sclerosis (MS) is a chronic immune-mediated disease of the central nervous system. While disease-modifying therapies can reduce relapse rates, their limitations have spurred interest in adjunctive approaches such as fasting and ketogenic diets (FD, KD). In a randomized controlled trial, participants with relapsing-remitting MS followed FD, KD, or a control diet for 9 months, with multi-omic and clinical assessments. KD primarily benefited MS via direct modulation of gut microbial function, enriching propionate production and glycerol metabolism modules linked to lower lesion volume. *Romboutsia timonensis, Roseburia intestinalis*, and *Bacteroides thetaiotaomicron* emerged as contributors, while KD shifted tryptophan metabolism toward microbiome-derived indoles, indicating functional rerouting along the gut-brain axis. Stool propionate did not reflect metagenomic potential, underscoring host and ecosystem complexity. We demonstrate novel evidence that KD drives tryptophan metabolism rerouting and species-specific functional reprogramming, mechanistically linking diet to neuroprotection and revealing new targets for microbiome-based MS therapies.

Registry: ClinicalTrials.gov, TRN: NCT03508414, Registration date: 25 April 2018

INTRODUCTION

Multiple sclerosis (MS) is a chronic immune-mediated disorder characterized by inflammatory demyelination, axonal damage, and plaque formation in the central nervous system (CNS) [1]. Globally affecting approximately 2.8 million individuals, MS exhibits a striking female predominance and typically manifests around the age of 30 [2]. While genetic predispositions contribute to susceptibility, environmental factors, including Epstein-Barr virus infection, vitamin D deficiency, smoking, and dietary patterns, influence disease onset and progression [3]. The pathophysiology involves autoreactive T-cells breaching the blood-brain barrier (BBB) and subsequently infiltrating the CNS, where they lead to myelin destruction [4]. This process disrupts neural signaling, resulting in motor, sensory, and cognitive impairments [5, 6].

While no cure for MS exists, disease-modifying therapies (DMTs) such as immunomodulators and monoclonal antibodies reduce relapse frequency and lesion formation [7]. However, these treatments often carry significant side effects and vary in efficacy depending on patient characteristics and disease progression [8]. This has spurred interest in adjunctive approaches like dietary interventions, which recent research suggests have the potential to enhance the efficacy of DMTs in MS management [9]. Nutritional interventions are of particular interest given epidemiological observations linking high-fat, high-carbohydrate Western dietary patterns to increased MS incidence [10]. While healthy, anti-inflammatory diets are broadly associated with improved general health, compelling evidence for a direct impact on MS disease pathology remains limited. Nonetheless, emerging research into fasting diets (FD) and ketogenic diets (KD) indicates that these interventions may confer mechanistic benefits relevant to MS [11, 12].

KDs, which are characterized by low-carbohydrate, high-fat intake, induce the production of ketone bodies such as 3-hydroxybutyric acid (3HB), which has been shown to reduce MS severity in established experimental autoimmune encephalomyelitis (EAE) mouse models [13, 14]. This protective effect occurs through enhanced myelination and reduced axonal degeneration [15]. Similarly, intermittent fasting has been shown to inhibit autoimmunity in EAE mice by increasing regulatory T-cell populations, reducing IL-17-producing T-cells, and enhancing gut microbial diversity [16]. In translating these findings to the clinical setting, Fitzgerald and colleagues found that calorie restriction and intermittent fasting led to significant weight loss and improved emotional well-being in individuals with MS [17]. Additionally, an 8-week intermittent fasting study showed a reduction in specific subsets of memory T cells, suggesting additional benefits beyond weight loss and emotional well-being [18]. A growing body of research suggests that KDs may be beneficial for MS patients when carried out for at least 6 months, demonstrating their safety and potential to improve fatigue, depression, and quality of life [19–22]. However, larger, randomized-controlled studies are needed to confirm these results.

Short-chain fatty acids (SCFAs) such as butyric acid and propanoic acid, produced by commensal bacteria fermenting dietary fiber, exhibit anti-inflammatory effects in both the gut and CNS [23]. They potentially modulate the gut-brain axis by protecting the BBB, reducing neuroinflammation and oxidative stress, and regulating cell cycle and apoptosis processes [24]. In MS patients' feces, however, they are notably depleted [25]. Addressing this depletion by improving propanoic acid levels in MS patients through supplementation has shown beneficial effects on immunological, neurodegenerative, and clinical outcomes in an uncontrolled study, potentially due to enhanced regulatory T cell differentiation [26, 27]. Tryptophan metabolism, which is orchestrated by gut microbes, is similarly disrupted in MS. Proinflammatory cytokines divert tryptophan toward the kynurenine pathway, generating neurotoxic quinolinic acid during relapses in MS patients [28, 29]. This conversion is facilitated by indoleamine 2,3-dioxygenase, which can be modulated by SCFAs such as butyrate [30]. Conversely, microbiome-derived indole derivatives have been reported to decrease neurodegeneration and inflammation in MS model mice, likely upon binding to the aryl hydrocarbon receptor in astrocytes [31].

Distinct microbial signatures further underscore the gut-brain axis's role in MS pathogenesis [32]. Fecal microbiota transplants from MS-discordant twins to germ-free mice exacerbate autoimmunity, directly confirming microbiome involvement in disease progression [33, 34]. Furthermore, KDs actively modulate these microbial communities in MS patients, leading to higher bacterial concentrations and diversity after 6 months [35]. This evidence highlights how dietary strategies may correct metabolite imbalances and microbial dysbiosis to influence MS outcomes. However, the precise effects of dietary interventions on microbial metabolism and metabolic potential in MS remain unclear.

To address the evidence gap, a large-scale, randomized controlled clinical trial has been designed to examine the effects of FD and KD in comparison to a standard healthy control diet (CD) in individuals with relapsing-remitting MS (RRMS) [36]. Stool and serum samples were collected at baseline and after 9 and 18 months, accompanied by analyses of patient-centered outcomes, including functional and self-reported outcomes. While pharmacological therapies remain the cornerstone of MS management, these

emerging dietary strategies offer a promising complementary approach that may ultimately lead to more holistic and effective disease management.

RESULTS

Baseline metabolic state shaped dietary response in MS patients

The Nutritional Approaches in Multiple Sclerosis (NAMS) study categorized patients with confirmed diagnosis of RRMS per 2017 McDonald criteria into three distinct dietary intervention groups: a primarily vegetarian Mediterranean diet (CD) following German Society for Nutrition guidelines, the same diet with intermittent fasting and a twice-yearly 7-day Buchinger fast (FD), and a KD restricting carbohydrates to 20–40 g/day while maintaining fat intake at 70–80% of total energy consumption (Fig. 1) [37]. Participants were eligible if they had stable or no DMT for at least six months, evidence of recent disease activity, and an EDSS score under 4.5, while recent changes in therapy served as key exclusion criteria (Supp. Table 1) [36]. Here, we include 76 patients who adhered to the study protocol for 9 months and provided stool and blood samples alongside anthropometric measurements, MRI-based data, and assessments of physical and mental health both at baseline and after 9 months of participation. Stool samples were collected to assess SCFA and tryptophan metabolite concentrations and to characterize the microbial community, while blood samples were used for parallel metabolomic analyses and additional health assessments, such as neurofilament light chain (NfL) concentration (Fig. 1).

The primary endpoint, the number of T2 lesions on brain MRI, did not change with any of the interventions as described by Bahr *et al.* [38]. Our measurement of 3HB corresponded to the values measured by the external diagnostic provider Labor Berlin (Fig. S1 A), thereby confirming the reproducibility of the data. The increase in the ketone bodies acetoacetic acid (AA) and 3HB was substantially higher in the KD group than in the other two groups, and none of the tested covariates confounded this result (Fig. S1 B, Fig. S2 A, Supp. Material 1). The impact of the different diets on the initial concentrations of AA, 3HB, hexanoic acid, and hydroxymethyl butyric acid (HMB) was also dependent on the baseline levels of these compounds. Patients with elevated initial levels of any of these compounds (+ 1 standard deviation (SD) from the mean) demonstrated no considerable variation in their metabolic response to dietary interventions. In contrast, patients within the KD cohort with low baseline values of AA, 3HB, and HMB (-1 SD from the mean) exhibited a substantial elevation relative to the FD group (Fig. 2A-C). For AA, this pattern was also observable at mean baseline levels and in comparison to the CD group (Fig. 2B).

KD led to a shift in tryptophan metabolism towards indole derivatives

In the KD group, serum tryptophan and its direct metabolite, kynurenine, both exhibited reductions, whereas the microbiome-derived indole-3-acetate (I3A) displayed a greater increase compared to the

other two groups (Fig. 3A, C). These results could not be attributed to the effects of other tested variables, although I3A was associated with age at each visit (Fig. S2 A, Supp. Table 1). Importantly, dietary tryptophan levels were not associated with serum tryptophan levels and thus did not confound the result (Fig. S2 B). The kynurenine metabolite 3-hydroxykynurenine did not show dietary group-dependent changes, though its levels tended to remain low after 9 months in the KD group, with a slight increase in the CD group and a slight decrease in the FD group (Fig. 3A). Levels of 5-hydroxytryptophan, a precursor in the serotonin pathway, decreased in both the CD and KD groups, but remained stable in the FD group; however, these differences were not statistically significant (Fig. 3B). Its downstream product, serotonin, did not exhibit group-dependent changes over time. The microbiome-related compounds indole-3-lactate (ILA) and trimethylamine N-oxide (TMAO) did not exhibit notable responses to the dietary interventions (Fig. 3C). However, the pattern observed in the ratio of each tryptophan metabolite to tryptophan revealed a significantly greater increase in the ratio of the two measured indoles to tryptophan in the KD group compared to the other two groups, with no confounding variables affecting this result (q_{I3A} = 0.002, q_{II A} = 0.004, Fig. S2 C).

Microbiome diversity remained stable despite dropout bias

Our metagenomic sequencing results revealed a dropout bias. Patients dropped out due to various factors, including medication changes, pregnancy, and non-compliance with the dietary protocol [38]. While the baseline Shannon diversity was not predictive of a patient dropping out of any of the interventions – that is, there was no significant difference in baseline alpha diversity between perprotocol and drop-out patients – the analyzed per-protocol cohort of patients in the KD group had considerably lower baseline Shannon diversity than per-protocol patients in the CD or FD groups (Fig. 4A). After identifying and quantifying this dropout-related bias, we systematically evaluated all subsequent analyses against it. To assess the potential effect of this difference on microbial dynamics within each intervention group, we estimated the probable alpha diversity for each dropout patient at 9 months using Multivariate Imputation by Chained Equations (MICE) and calculated the resulting change in diversity. These changes did not differ between MICE-imputed drop-out patient and per-protocol patient data (Fig. 4B). Similarly, the diets did not lead to a shift in beta diversity ($p_{PERMANOVA} = 0.4$). However, KD was associated with depletion of the *Bifidobacterium* genus compared to FD and CD ($q_{KDvsFD} = 0.001$, $q_{KDvsCD} = 0.044$, $q_{CDvsFD} = 0.403$, Fig. 4C, D).

Microbiome functional and compositional contributions to lesion outcomes differed across diets

We used the same approach for gut microbial modules (GMMs) to identify microbial functional entities directly associated with the dietary interventions, that is, without confounding factors [39]. The ketogenic diet enriched the GMMs glycerol degradation III (MF0062) and propionate production II (MF0094) to a greater extent than the other two diets (Fig. 5A). In contrast, starch degradation (MF0005) and sucrose

degradation II (MF0011) were reduced in the KD group compared to the other two groups (Fig. 5A). We then examined whether these changes had a group-dependent influence on lesion count or volume, insulin-like growth factor 1 (IGF1) concentration, NfL concentration, symbol digit modalities test (SDMT) results, or Beck depression inventory II (BDI-II) score. Indeed, changes in starch degradation (MF0005) had a differential influence on lesion count that varied between the groups, with increasing abundance of this GMM being correlated with a decrease in lesion count in the FD group specifically (Fig. 5B). Additionally, the enrichment of propionate production II (MF0094) was associated with a steeper decrease in lesion volume in KD than in FD and CD. We next investigated whether specific microbial species were responsible for this association. To achieve this, we examined which species exhibited associations mirroring the relationship between a GMM and lesion volume and count. Ten species showed time- and group-dependent relationships with lesion volume and count (q < 0.1) and were therefore tested for analogous links to group-associated GMMs. Three of these species – *Romboutsia* timonensis, Roseburia intestinalis, and Bacteroides thetaiotaomicron – elevated propionate production II (MF0094) to a greater extent in KD than in the other two diets (Fig. 5C). Similarly, *Intestinibacter bartlettii* displayed a stronger positive association with starch degradation (MF0005) in KD than in the other two diets and was uniquely associated with decreasing lesion count in the FD group alone (Fig. 5C & Fig. S3). These species' temporal dynamics with both GMMs and outcome metric aligned directionally (Fig. 5 & Fig. S3).

Microbial propionate pathway dynamics varied by diet

Propionate production II (MF0094) comprises only one KEGG orthologue (KO) (K01026, EC:2.8.3.1), which corresponds to propionate CoA-transferase. This enzyme is an integral part of propionate metabolism, primarily transferring CoA from propionyl-CoA to acetate, thereby producing propionate and acetyl-CoA. It has also been shown to transfer CoA to and from other carboxylic acids, such as butyrate, in various taxa [40]. Given this broad enzymatic activity, we examined whether stool levels of acetate, butyrate, and propionate differed among the diet groups. Although no statistically significant differences were detected, there was a trend toward lower propionate levels in the KD group and lower butyrate levels in the FD group (Fig. S4). Next, we tested whether these metabolites reflect the metabolic dynamics of this microbial footprint, independent of the group. Stool acetate, butyrate, and propionate showed no temporal association with propionate production II (MF0094) and lacked group-dependent associations with lesion volume (Fig. 6A-B). However, propanoic acid exhibited group-independent temporal correlations with two of the previously identified species, R. intestinalis and B. thetaiotaomicron, showing stronger positive associations with propionate production II (MF0094) across visits in KD compared to CD and FD (Fig. 6C). Acetic acid exhibited this pattern solely with R. intestinalis (Fig. 6C). We applied the same analytical framework to investigate whether temporal shifts in tryptophan metabolism within the KD group were linked to propionate production II (MF0094) dynamics. Among the four diet-associated serum tryptophan metabolites, kynurenine and tryptophan demonstrated decreasing levels that were concurrent with rising propionate production II (MF0094), irrespective of intervention group (Fig. 6D). Moreover, the relationship between changing levels of these metabolites and lesion

volume changes was stronger and more positive in the KD group compared to CD and FD (Fig. 6E). These metabolites shared no synchronous temporal pattern with any species linked to propionate production II (MF0094) dynamics (Fig. 6F). Furthermore, mediation analysis revealed that propionate production II (MF0094) abundance exhibited patterns consistent with mediation of the effect of KD on lesion volume (Fig. S5).

DISCUSSION

Our findings suggest that the beneficial effects of KD are largely mediated by its direct modulation of gut microbiome function, as evidenced by its pronounced impact on the abundance of four GMMs and the observed relationship between propionate production potential and lesion volume in MS. The negative correlation is significantly stronger under KD than under the other diets, suggesting that this microbial module may confer a protective effect on lesion dynamics specifically with KD. Alongside propionate production II (MF0094), glycerol degradation III (MF0062) is enriched in the KD group. This GMM includes key enzymes, glycerol dehydratase and 1,3-propanediol dehydrogenase, that mediate the microbial conversion of glycerol to 1,3-propanediol. This process is critical for microbial redox balance, as it regenerates NAD+. As KD involves increased fat intake, more glycerol is derived from fat metabolism, providing a substrate for microbial fermentation and redox homeostasis. At the same time, the depletion of starch and sucrose degradation modules under KD likely reflects carbohydrate scarcity. These shifts collectively indicate that the gut microbiome adapts to the available substrate landscape under KD, redirecting metabolism to maintain energy production and redox balance, and increasing the genetic capacity for propionate production [41, 42]. Given that propionate has been implicated in neuroprotective roles in MS, this functional shift and its positive effect on lesion volume in KD may be of clinical relevance [27].

Three anaerobic SCFA-producing species, *R. timonensis*, *R. intestinalis*, and *B. thetaiotaomicron*, might be involved in the KD-specific protective effect of propionate production II (MF0094) on lesion dynamics over time. In the context of KD, these species show a stronger positive association with propionate production II (MF0094) counts and a stronger negative association with lesion volume compared to the other diets. The absence of this effect in lesion counts may be attributed to limitations in detection sensitivity or reflect KD's role in myelin regeneration within the intricate de- and remyelination processes of inflammatory lesions, as opposed to the inhibition of de novo lesion development [43]. Additionally, the lack of association with lesion counts could be influenced by the presence of vascular lesions, which contribute to total lesion volume but may not be related to inflammatory demyelinating activity [44]. This implies that KD positively influences a dynamic microbiota-brain link, particularly shaped around propionate metabolism and redox balancing under carbohydrate scarcity.

Under FD, periodic nutrient shortages trigger dynamic shifts in the gut microbiome, making lesion count a stronger negative correlate of both starch-degradation capacity and *I. bartlettii* [45, 46]. The strong negative association between *I. bartlettii* and starch degradation (MF0005) under KD, a diet marked by a persistent decline in community-wide starch degradation capacity, highlights *I. bartlettii*'s sensitivity to

carbohydrate availability fluctuations [47]. This pattern also reflects the species' neuroprotective role in high-competition settings that still require some carbohydrate use, potentially through its ability to produce propionate [48, 49].

Stool metabolomics, however, revealed no correlation between stool propionate and propionate production II (MF0094) counts regardless of the diet. Our data rather pointed to a trend toward decreased fecal propionate levels under KD, which has been reported previously for short-term KD [50, 51]. Serum propionate levels were undetectable, likely due to common difficulties in SCFA measurement, including their high volatility [52]. This discrepancy raises the guestion of whether fecal SCFA assessments accurately reflect intestinal production or rather represent residual metabolites not absorbed by the host. There is evidence showing that fecal SCFA concentrations are influenced by various factors, including the rate of microbial production, gut transit time, the efficacy of host absorption, and even the country of residence of a patient [53–55]. The observed associations between propionate and acetate levels and microbial species exhibiting KD-specific neuroprotective effects, however, highlight that the coordinated metabolic contributions of multiple microbial taxa may drive the link between microbial propionate metabolism and lesion volume under KD. The strong, diet-independent correlations between propionate production II (MF0094) and serum tryptophan and kynurenine, alongside the observation that under KD their depletion is associated with reduced lesion volume, underscore the complexity of these metabolic interactions. Together with the mediating role of propionate production II (MF0094) between diet and lesion volume, these findings suggest that propionate production II (MF0094) may serve as a proxy for the overall fermentative capacity and functional state of the gut microbiome, rather than solely reflecting SCFA production.

Many patients on KD were indeed in a ketotic state, as shown by the strongly elevated ketone body levels in the KD group. That the production of ketone bodies and SCFAs in response to KD in particular depended on their baseline values suggests that the efficacy of a diet is limited and tied to parameters such as previous levels of ketogenesis and SCFA production, possibly induced by preceding dietary patterns. KD is a particularly challenging nutritional regimen, which might explain why it displayed a larger potential for a metabolic shift than FD in individuals with below-average starting levels of SCFAs and ketone bodies [56]. Research has indicated that a physiological limit for ketone body production and utilization exists, possibly depending on the body's capacities and energy needs [57]. Also, factors such as the apolipoprotein E4 genotype, habitual physical exercise, and health parameters such as kidney or cardiovascular conditions have been shown to influence the body's response to calorie restriction [58–61]. Therefore, recommendations for KD should not only account for underlying health conditions but also recognize that individuals with a diet already leading to high SCFA and ketone body levels may gain minimal advantages from a switch to KD [62].

Evidence has already shown that the KD affects the human metabolome, tryptophan degradation to kynurenine and downstream metabolites in particular: while one study showed increased levels of kynurenine and decreased levels of quinolinic acid in urine, another study showed reduced levels of kynurenine in the plasma and hippocampus of KD-fed rats [63, 64]. Since the kynurenine-to-tryptophan

ratio does not differ significantly between groups in our cohort, the observed decrease in tryptophan in the KD group is not explained by increased flux through the kynurenine pathway. Additionally, dietary tryptophan intake did not differ between groups and was not correlated with plasma tryptophan levels, indicating that dietary consumption is not responsible for the reduced tryptophan in KD. Therefore, we infer that the missing tryptophan in KD is likely diverted into other metabolic pathways, most plausibly the indole pathway, as evidenced by a steep increase in the ratio of the two measured indoles to tryptophan in the KD group only. Since indoles are produced by gut microbiota, this metabolic shift likely reflects changes in microbial community function rather than the abundance of individual bacterial species, as the depletion of *Bifidobacterium* in KD participants initially appears counterintuitive, given that this genus both ferments SCFAs and produces ILA [65, 66]. However, this reduction is welldocumented in KD studies and appears independent of fiber intake in our cohort, as fiber intake did not confound our result and was not significantly reduced in KD compared to the other two diets [67]. Therefore, the elevated levels of ketone bodies in our KD cohort may inhibit *Bifidobacterium* growth, which could also account for the absence of these effects in the FD and CD groups. This mechanism has been previously described and, coupled with increased availability of ILA, has been linked to reduced intestinal Th17 cell levels and lower inflammation [68, 13, 69, 70].

Our findings indicate that the beneficial effects of dietary interventions such as KD and FD in MS are likely mediated through complex, diet-specific shifts in microbial metabolic function, rather than changes in single taxa or SCFA concentrations alone. The metabolic potential, encoded through functional modules shared by consortia of diverse bacterial taxa, integrates signals from the gut microbial community and multiple pathways, reflecting the role of several species acting as key mediators of gutbrain communication, neuroimmune regulation, and disease progression. To our knowledge, this is the first report in MS to link diet-specific enrichment of a defined microbial functional module, propionate production II (MF0094), with improvements in MRI-derived lesion metrics, thereby positioning functional capacity as a proximate mechanistic correlate of neuroinflammatory outcomes. Critically, the efficacy and safety of such interventions are likely to depend on an individual's baseline microbiota composition, metabolic status, and capacity to adapt to nutritional stress. Thus, a nuanced understanding of these personalized responses will be crucial for refining dietary recommendations and leveraging gut microbiome function to optimize clinical outcomes.

METHODS

Sample acquisition

The NAMS study was registered at ClinicalTrials.gov under NCT03508414 and followed all relevant ethical regulations, including compliance with the Declaration of Helsinki. The ethics committee of Charité - Universitätsmedizin (EA1/200/16) approved the study protocol, and informed consent was obtained from all participants. As described by Bahr *et al.*, the cohort comprised adults with RRMS, an EDSS score below 4.5, and recent disease activity (≥ 1 new MRI lesion or clinical relapse in the previous two years), who were on stable or no DMT for at least six months prior to enrolment (Supp. Table 1) [36,

38]. Cerebral MRI scans were acquired at baseline and at 9 months using standardized 3D T1-weighted MPRAGE and 3D FLAIR sequences, with images co-registered to baseline in MNI space. T2-hyperintense lesions were manually segmented by two blinded, experienced raters. Lesion count and total lesion volumes were extracted from binary masks using FSL tools. Blood serum in plain tubes and whole stool samples from 76 per-protocol patients were acquired from the NAMS study and stored at -80°C. Additionally, 29 stool samples from drop-out patients were acquired. Stool samples were homogenized using an in-house-produced device (Fig. S6). This stool homogenization apparatus comprised a lever with a handlebar that could be affixed to two primary stainless-steel components: a reservoir and a lid. Before use, both components were frozen at -80°C. They maintained a sufficiently low temperature for approximately one hour, facilitating the sequential homogenization of frozen whole stool samples. The stool homogenization process was conducted under a fume hood equipped with a HEPA filter (Waldner, Germany). Each stool sample was retrieved from the freezer and promptly transferred to a sterile Whirl-Pak® Standard Sterilized Sampling Bag (Whirl-Pak, Madison, WI, USA), which was then placed in the reservoir situated on dry ice to ensure continuous cooling. The reservoir was positioned beneath the lid, and a safety pin securing the handlebar to the attached lid was removed. The lid was then lowered onto the sample (Fig. S6). To achieve homogenization, the handlebar was manipulated to move the lid in a vertical motion until the sample was thoroughly pulverized. The pulverized sample was aliquoted, and any remaining material was returned to the original sample container. The apparatus aperture was sanitized with ethanol before processing the next sample. Cooling remained sufficient for up to 1.5 hours. After this time, the reservoir and the lid were frozen at -80°C for at least 20 hours again.

Metabolomics measurement

Tryptophan metabolites measurement

In this study, 152 serum and 143 fecal samples underwent analysis over 3 batches. Concurrent quantification of 34 tryptophan metabolites and 9 branched-chain amino acids in two separate assays was conducted using a methanol extraction method with a 90% concentration [71]. The mobile phase system consisted of two components: Phase A, comprising 0.2% formic acid in water, and Phase B, consisting of 0.2% formic acid in methanol. Fecal samples were prepared by dissolving them in water to achieve a concentration of 50 mg_{Stool}/mL . For the extraction process, 50 μL of the biological sample was combined with 100 µL of a chilled solution containing 90% methanol, 0.2% formic acid, and 0.02% ascorbic acid, along with internal standards as described elsewhere [72]. The extraction protocol involved vortexing the samples for 30 seconds, followed by centrifugation at 1000 rpm for 10 minutes at 4°C, and incubation at -20°C for 1 hour. Subsequently, the samples were centrifuged again at 12,000 rpm for 10 minutes at 4°C. The analysis was performed using an Agilent 1290 ultra-high performance liquid chromatograph (UHPLC) system coupled to a Thermo Quantiva triple quadrupole mass spectrometer operating in multiple reaction monitoring (MRM) mode. Chromatographic separation was achieved using a Waters XSelect Premier HSS T3 column (2.5 µm, 2.1 × 150 mm) with a 10-minute gradient at around 400 bar, a flow rate of 0.4 mL/min, and an injection volume of 5 µL. The gradient program was as follows: starting at 97% A/3% B and maintaining these conditions for 0.45 minutes, transitioning to 70%

A/30% B at 1.2 minutes, then to 40% A/60% B by 2.7 minutes (held until 3.75 minutes), followed by a transition to 5% A/95% B at 4.5 minutes (maintained until 6.6 minutes), and finally returning to the initial conditions at 6.75 minutes with re-equilibration until 10 minutes. A calibration curve consisting of a mix of 34 tryptophan standards plus TMA and TMAO was run at 11 concentrations in the matrix background of charcoal-stripped plasma. Level 6 of this mix and a solvent blank were run every 6 samples as an extra quality check. Pooled quality control samples (QCs) were prepared by pooling all of the samples and run at the beginning, end, and every 6 samples during each batch. 6 extracted charcoal-stripped plasma samples were run before 6 extracted water samples at the end of the sequence.

Short-chain fatty acid and ketone body measurement

For the simultaneous quantification of eight SCFAs and two ketone bodies, an analytical method employing 3-nitrophenylhydrazine (3NPH) derivatization was used [73]. Stool aliquots were dissolved in a 50% acetonitrile:water solution to reach a concentration of 33.33 mg_{Stool}/mL. The samples were homogenized using a FastPrep, centrifuged, and the supernatant was collected. Sample preparation involved mixing 40 µL of serum or stool supernatant with 20 µL of 200 mM 3NPH, 20 µL of 120 mM N-(3dimethylaminopropyl)-N'-ethylcarbodiimide (EDC) containing 6% pyridine, and 10 µL of 50 µM isotopelabeled internal standards. The derivatization reaction was carried out at 40°C for 45 minutes, followed by dilution with 410 µL of 10% acetonitrile:water and centrifugation at 6600×g for 10 minutes at 20°C. The supernatants were then transferred to brown glass vials for immediate UPLC-MS/MS analysis. The UPLC-MS/MS system consisted of an Agilent 1290 Infinity II UPLC coupled to a ThermoFisher TSQ Quantiva triple quadrupole mass spectrometer. Chromatographic separation was performed using a Waters ACQUITY BEH C18 column (1.7 µm, 2.1 × 100 mm) maintained at 40°C with a 5 µL injection volume. The mobile phase comprised water with 0.1% formic acid (Phase A) and acetonitrile with 0.1% formic acid (Phase B) at a flow rate of 0.3 mL/min. An optimized gradient was implemented as follows: 5% B for 5 minutes, 5–55% B over 12 minutes, 100% B for 1 minute, followed by 2 minutes at 5% B. Multiple reaction monitoring (MRM) was performed in negative electrospray ionization mode with a spray voltage of 2500 V, an ion transfer tube temperature of 342°C, and a vaporizer temperature of 300°C. Quality control samples, as described previously, were also employed in this analysis.

Metabolomics data processing

Data processing per matrix and method utilized *Skyline* software (v. 22.2.0.527) for peak integration and quantification, as well as R (v. 4.2.3). Peaks were normalized to corresponding internal standards. Metabolite areas were retained if they were quantifiable or fell between the limit of detection and the lower limit of quantification in at least 60% of samples across all statistical groups. Batch correction was performed using pooled QC sample-based robust locally estimated scatterplot smoothing signal correction from the statTarget package (v. 1.28.0) with a smoothing parameter set to 0.75 [74, 75]. Missing stool tryptophan values (n = 13) were imputed using half minimum value imputation. Compound retention required that the relative standard deviation (RSD) of QCs did not exceed 60% in stool and 30% in serum. Only metabolites with a per batch biological sample RSD within samples that was at least 20% larger than the per batch RSD measured in QCs for that batch in all batches were used in the analysis.

Stool metagenomic sequencing

DNA was extracted using the ZymoBIOMICS-96 MagBead DNA Kit (Zymo Research Europe GmbH, Freiburg, Germany) in the automated system TECAN Fluent® 780 NAP workstation following the manufacturer's instructions with minimal modifications to the lysis step. 100 mg of the homogenized fecal material and 750 µl of lysis buffer were used for mechanical and chemical lysis using a PeQLab Precellys 24 (Bertin Corp., Rockville, MD, USA) for 2×15 s at 5500 rpm for a total of three mechanical lysis cycles. The DNA was eluted in 50 µL of ZymoBIOMICS DNase/RNase Free Water. Samples were randomized, and both negative and positive controls were included at each extraction batch. Concentration was measured using Qubit dsDNA Broad Range Kit (Thermo Fisher Scientific, Walham, USA), revealing 135 samples with sufficient DNA concentration. Samples were stored at -80°C before shipment to NovoGene for metagenomic sequencing. Shotgun sequencing of 150 bp paired-end reads was performed on the Illumina NovaSeq 6000.

Metagenomic profiling and diversity imputation Taxonomic and functional profiling of metagenomic data

Raw metagenomic sequencing data were processed using customized scripts with the *NGLess* framework (v. 1.5) [76]. Quality control and filtering steps removed reads below a minimum quality score of 25 and a read length threshold of 45 bp. Human DNA contamination was filtered by alignment to the GRCh38.p13 genome (masked with ProGenomes3 database parameters, requiring \geq 45 bp matches and \geq 90% identity). Taxonomic profiling of bacterial species was performed using *mOTUs* (v. 3) [77]. Functional profiles based on the Kyoto Encyclopedia of Genes and Genomes (KEGG) [78] were obtained by mapping to the Global Microbial Gene Catalog (GMGC) (v. 1) [79], binned to KOs, and normalized to fragments per kilobase of gene per million reads mapped (FPKM).

Alpha diversity imputation

MICE with predictive mean matching over 100 iterations was used to impute alpha diversity values for drop-out patients at visit three. The *mice* package (v. 3.17) was utilized to identify per-protocol patients within the same group for each dropout patient, ensuring they had a comparable predicted final alpha diversity based on regression modelling [80]. The imputed value was then randomly selected from the final alpha diversity values actually observed in the respective set of per-protocol patients, preserving the original data structure.

Metagenomic sequencing data processing

Our analysis was based only on mOTUs with a prevalence above 50% in one intervention group, or a relative abundance of at least 0.01%. The filtered table was subsequently utilized to aggregate mOTUs that are part of a higher-level taxon, facilitating the analysis of higher-level taxon abundance. The *omixRpm* package (v. 0.3.3), applying the human gut metabolic modules database by Vieira-Silva *et al.*

and a minimum pathway coverage of 0.3, was used to aggregate KEGG KOs to GMMs [39, 81]. KOs and GMMs were filtered analogously.

Statistical analysis

Model-based group comparisons and confounder identification

All statistical analyses were performed using R (v. 4.4.2). To evaluate the differences between groups regarding the feature development's dependence on its baseline levels, the *interaction* package (v. 1.2.0) was used [82]. The slope of each group at different values of the logged feature baseline values was calculated using standard values for continuous moderators, specifically its mean and +/- 1 SD [83]. This was done within a linear model with restricted maximum likelihood using the *lme4* package (v. 1.1–35.5) and accounting for interaction effects between intervention and baseline feature values on feature percent changes [84]. Resulting p-values for AA, 3HB, HMB, and hexanoic acid were FDR-adjusted over all four tested metabolites and all group and interval comparisons. All tryptophan metabolites, which were measured in serum and passed QC, were tested for an association with group by linearly modelling their log AUCs with a group-time interaction while accounting for repeated measures and estimating parameters via maximum likelihood, before testing whether the interaction term reduced the residual sum of squares significantly using a Chi-square test with both nested models. The conditional \mathbb{R}^2 for each model was calculated using the MuMIn package (v. 1.48.4) and used to determine Cohen's f^2 . The same approach was applied to all covariates by systematically changing the model to a covariate-time interaction. Results were FDR-adjusted over tested features, and compounds associated with the diet group, i.e., with a q-value of 0.1, were tested for confounding with covariates, which similarly reached a qvalue of 0.1 for that compound (Supp. Material 1): a model with both interaction terms, group-time and covariate-time, was constructed, and the contribution of each interaction term to the model was evaluated as described above. If the covariate-time interaction added significant predictive value to the model (p < 0.1) while the group-time did not (p > 0.1), the covariate was considered to confound the group association of the compound. The same approach was applied to ranked taxon counts and GMMs, additionally using microbial alpha diversity and the first and second principal coordinate axes calculated as described above. Post hoc tests for significant features were performed by computing estimated marginal means using the emmeans package (v. 1.10.5) [85]. For metabolic features, p-values for pairwise comparisons were adjusted using the multivariate t distribution. For ranked metagenomic features, the same framework was applied, but the Dunn procedure was used for p-value adjustment.

Alpha and beta diversity assessment

Alpha diversity metrics (Shannon diversity, Chao1 richness, and Simpson's evenness) were calculated using the *microbiome* package (v. 1.28.0) after rarefaction to an even depth of 4000 reads per sample using the *phyloseq* package (v. 1.52). Differences in Shannon alpha diversity were assessed using a Kruskal-Wallis test with a subsequent Dunn's test for post-hoc group effect evaluation. The *vegan* package (v. 2.6-8) was used to compute the Bray-Curtis distance for compositional analysis [86]. To

evaluate the compositional differences between samples at the genus level, principal coordinate analysis using Euclidean distance and k = 2 dimensions was conducted. A PERMANOVA using 999 permutations constrained within repeated measures was employed to test for group differences.

Assessing diet-dependent predictors of MS outcomes

The group-dependent predictive value of a feature for different MS disease outcomes examined in the NAMS study - IGF1 concentration, NfL concentration, MRI T2 lesion volume, T2 lesion count, SDMT, and BDI-II score – was assessed by linearly modelling the outcome variable in response to the three-way interaction between group, time, and feature while accounting for inter-patient variability. Only the threeway interaction term was tested for significance in a Chi-squared test, as described above. KD was used as the reference level. The sign of the estimate of each interaction term for the other diet groups was used to determine the direction of the effect size, Cohen's f^2 , calculated from the conditional R^2 of both models. This resulted in two versions of f^2 – positive or negative – corresponding to the two alternative diet groups. Benjamini-Hochberg adjustment for multiple testing was performed across all tested combinations, and the significance threshold was set to q < 0.1. This analysis was conducted in a hypothesis-driven manner for group-associated GMMs ($n_{lesion\ volume}$ = 134). To identify species related to the GMM-related outcomes, this procedure was repeated in a hypothesis-generating manner for all species and these GMM-related outcomes. To determine which of the outcome-related species (q < 0.1) follow the group-dependent GMM-outcome trajectory, the respective ranked GMM abundances were modelled with each of these species as a predictor in the same way, applying a three-way interaction between species, time, and group before adjusting for all GMM-species combinations.

Cross-omics linear modelling

To investigate whether two features from different omics domains develop simultaneously over all groups, we linearly modelled one feature using the other (e.g., log abundance of metabolites from microbial features, ranked GMMs from taxa) while accounting for group and time. A likelihood ratio test (Chi-square) was applied to two nested models to assess the significance of the predictive feature term in the full model. The sign of the estimate of the tested fixed effect feature determined the directionality of f^2 . Benjamini-Hochberg adjustment for multiple testing was performed across all tested combinations. Only samples with results for both omics domains in question were used for multi-omics analysis.

Mediation analysis framework

The *mediation* package (v. 4.5.0) was applied to test for mediation effects [87]. These indirect effects were estimated via 10,000 Monte Carlo simulations, with significance determined by 95% bias-corrected confidence intervals. The dataset was filtered to contain only two diet groups at a time (KD vs. CD, KD vs. FD, and CD vs. FD) to account for group-to-group mediation differences. To test whether a group-associated feature mediated the effect of the diet group on another feature or an outcome, two linear

mixed-effects models were constructed. One modelled the feature using fixed effects for visit, diet group, and their interaction, with a random intercept per patient to account for repeated-measure correlations and baseline variability between individuals. The second modelled the other feature or outcome with the same fixed effects and interaction term, adding the previous feature's abundance. The group was used as the treatment variable, and the metabolite or taxon was considered the mediator. When tested as potential mediators, metabolite abundances were logged, and taxonomic features were ranked. The effect size was calculated as the absolute value of the average causal mediation effect (ACME) divided by the sum of the absolute values of the ACME and the average direct effect (ADE). Benjamini-Hochberg adjustment for multiple testing was performed across all tested combinations if applicable.

Artificial intelligence use

Claude Sonnet (Anthropic) was used to assist with manuscript writing and coding for data analysis; Perplexity was used to conduct literature searches and contextualize findings within existing research. All artificial intelligence contributions were thoroughly reviewed and validated by the authors, who retain full responsibility for the scientific content, methodology, and conclusions.

Declarations

ADDITIONAL INFORMATION

All authors declare no financial or non-financial competing interests.

Author Contribution

F.P., J.B., and L.B. planned and conducted the NAMS study. L.M. coordinated timelines and sample logistics. J.K., U.B., and F.G. planned the metabolomics experiments and designed the stool crusher. U.B. and F.G. conducted the metabolomics experiments. V.D. and F.G. planned and conducted the metagenomic sequencing experiments. F.G. processed and cleaned the metabolomics datasets and metadata. F.G. analyzed the results, visualized the data, and wrote the original draft. L.B. and R.R. conducted the study visits. F.P., L.B., M.W., and S.J. guided the interpretation of results. J.K. and S.F. supervised this work. All authors reviewed the manuscript.

Acknowledgement

The authors thank Stefan Jordan, Chotima Böttcher, Sarah Trajkovski, Janine Wiebach, and Daniela Sofia Bastos Dias for their continued support throughout this project. Some of the icons in Fig. 1 were sourced from svgRepo.com (public domain, no attribution required). This study was funded by the Walter and Ilse Rose Foundation and the Myelin Project. F.G. received funding from the central MDC budget. S.F.

received funding from the Horizon Europe project "IMMEDIATE" (grant number 101095540). The funder played no role in study design, data collection, analysis and interpretation of data, or the writing of this manuscript.

Data Availability

The code and individual participant data underlying the results of this article are not publicly available due to privacy and ethical considerations. However, they will be shared after de-identification and subject consent with researchers who provide a methodologically sound proposal on a related research question.

References

- 1. Dendrou, C. A., Fugger, L. & Friese, M. A. Immunopathology of multiple sclerosis. *Nature Reviews Immunology* 15, 545–558 (2015).
- 2. Gold, S. M., Willing, A., Leypoldt, F., Paul, F. & Friese, M. A. Sex differences in autoimmune disorders of the central nervous system. *Semin Immunopathol* 41, 177–188 (2019).
- 3. Ramagopalan, S. V., Dobson, R., Meier, U. C. & Giovannoni, G. Multiple sclerosis: risk factors, prodromes, and potential causal pathways. *The Lancet Neurology* 9, 727–739 (2010).
- 4. Liu, R. *et al.* Autoreactive lymphocytes in multiple sclerosis: Pathogenesis and treatment target. *Front. Immunol.* 13, 996469 (2022).
- 5. Lublin, F. D. *et al.* How patients with multiple sclerosis acquire disability. *Brain* 145, 3147–3161 (2022).
- 6. Benedict, R. H. B., Amato, M. P., DeLuca, J. & Geurts, J. J. G. Cognitive impairment in multiple sclerosis: clinical management, MRI, and therapeutic avenues. *Lancet Neurol* 19, 860–871 (2020).
- 7. Amin, M. & Hersh, C. M. Updates and Advances in Multiple Sclerosis Neurotherapeutics. *Neurodegenerative Disease Management* 13, 47–70 (2023).
- 8. Lee, C.-Y. & Chan, K.-H. Personalized Use of Disease-Modifying Therapies in Multiple Sclerosis. *Pharmaceutics* 16, 120 (2024).
- 9. Jayasinghe, M. et al. The Role of Diet and Gut Microbiome in Multiple Sclerosis. Cureus 14, e28975.
- 10. Saresella, M. *et al.* Immunological and Clinical Effect of Diet Modulation of the Gut Microbiome in Multiple Sclerosis Patients: A Pilot Study. *Front. Immunol.* 8, (2017).
- 11. Harirchian, M. H., Karimi, E. & Bitarafan, S. Diet and disease-related outcomes in multiple sclerosis: A systematic review of clinical trials. *Current Journal of Neurology* 21, 52 (2022).
- 12. Storoni, M. & Plant, G. T. The Therapeutic Potential of the Ketogenic Diet in Treating Progressive Multiple Sclerosis. *Mult Scler Int* 2015, (2015).
- 13. Alexander, M. *et al.* A diet-dependent host metabolite shapes the gut microbiota to protect from autoimmunity. 2023.11.02.565382 Preprint at https://doi.org/10.1101/2023.11.02.565382 (2023).

- 14. Choi, I. Y. *et al.* A Diet Mimicking Fasting Promotes Regeneration and Reduces Autoimmunity and Multiple Sclerosis Symptoms. *Cell Reports* 15, 2136–2146 (2016).
- 15. Mu, J. *et al.* Ketogenic diet protects myelin and axons in diffuse axonal injury. *Nutr Neurosci* 25, 1534–1547 (2022).
- 16. Cignarella, F. *et al.* Intermittent Fasting Confers Protection in CNS Autoimmunity by Altering the Gut Microbiota. *Cell Metabolism* 27, 1222–1235.e6 (2018).
- 17. Fitzgerald, K. C. *et al.* Effect of intermittent vs. daily calorie restriction on changes in weight and patient-reported outcomes in people with multiple sclerosis. *Mult Scler Relat Disord* 23, 33–39 (2018).
- 18. Fitzgerald, K. C. *et al.* Intermittent calorie restriction alters T cell subsets and metabolic markers in people with multiple sclerosis. *eBioMedicine* 82, (2022).
- 19. Brenton, J. N. *et al.* Pilot study of a ketogenic diet in relapsing-remitting MS. *Neurol Neuroimmunol Neuroinflamm* 6, e565 (2019).
- 20. Brenton, J. N. *et al.* Phase II study of ketogenic diets in relapsing multiple sclerosis: safety, tolerability and potential clinical benefits. *J Neurol Neurosurg Psychiatry* 93, 637–644 (2022).
- 21. Lee, J. E. *et al.* A Modified MCT-based Ketogenic Diet Increases Plasma β-Hydroxybutyrate but has Less Effect on Fatigue and Quality of Life in People with Multiple Sclerosis Compared to a Modified Paleolithic Diet: A Waitlist-Controlled, Randomized Pilot Study. *J Am Coll Nutr* 40, 13–25 (2021).
- 22. Bock, M., Steffen, F., Zipp, F. & Bittner, S. Impact of Dietary Intervention on Serum Neurofilament Light Chain in Multiple Sclerosis. *Neurol Neuroimmunol Neuroinflamm* 9, e1102 (2022).
- 23. Barcutean, L., Maier, S., Burai-Patrascu, M., Farczadi, L. & Balasa, R. The Immunomodulatory Potential of Short-Chain Fatty Acids in Multiple Sclerosis. *Int J Mol Sci* 25, 3198 (2024).
- 24. Dong, Y. & Cui, C. The role of short-chain fatty acids in central nervous system diseases. *Mol Cell Biochem* 477, 2595–2607 (2022).
- 25. Zeng, Q. *et al.* Gut dysbiosis and lack of short chain fatty acids in a Chinese cohort of patients with multiple sclerosis. *Neurochemistry International* 129, 104468 (2019).
- 26. Haghikia, A. *et al.* Dietary Fatty Acids Directly Impact Central Nervous System Autoimmunity via the Small Intestine. *Immunity* 43, 817–829 (2015).
- 27. Duscha, A. *et al.* Propionic Acid Shapes the Multiple Sclerosis Disease Course by an Immunomodulatory Mechanism. *Cell* 180, 1067–1080.e16 (2020).
- 28. Lim, C. K. *et al.* Kynurenine pathway metabolomics predicts and provides mechanistic insight into multiple sclerosis progression. *Scientific Reports* 7, 41473 (2017).
- 29. Staats Pires, A. *et al.* Dysregulation of the Kynurenine Pathway in Relapsing Remitting Multiple Sclerosis and Its Correlations With Progressive Neurodegeneration. *Neurol Neuroimmunol Neuroinflamm* 12, e200372 (2025).
- 30. Martin-Gallausiaux, C. *et al.* Butyrate Produced by Commensal Bacteria Down-Regulates Indolamine 2,3-Dioxygenase 1 (IDO-1) Expression via a Dual Mechanism in Human Intestinal Epithelial Cells.

- Front Immunol 9, 2838 (2018).
- 31. Rothhammer, V. *et al.* Type I interferons and microbial metabolites of tryptophan modulate astrocyte activity and CNS inflammation via the aryl hydrocarbon receptor. *Nat Med* 22, 586–597 (2016).
- 32. Dunalska, A., Saramak, K. & Szejko, N. The Role of Gut Microbiome in the Pathogenesis of Multiple Sclerosis and Related Disorders. *Cells* 12, 1760 (2023).
- 33. Berer, K. *et al.* Gut microbiota from multiple sclerosis patients enables spontaneous autoimmune encephalomyelitis in mice. *PNAS* 114, 10719–10724 (2017).
- 34. Cekanaviciute, E. *et al.* Gut bacteria from multiple sclerosis patients modulate human T cells and exacerbate symptoms in mouse models. *PNAS* 114, 10713–10718 (2017).
- 35. Swidsinski, A. *et al.* Reduced Mass and Diversity of the Colonic Microbiome in Patients with Multiple Sclerosis and Their Improvement with Ketogenic Diet. *Front. Microbiol.* 8, (2017).
- 36. Bahr, L. S. *et al.* Ketogenic diet and fasting diet as Nutritional Approaches in Multiple Sclerosis (NAMS): protocol of a randomized controlled study. *Trials* 21, 3 (2020).
- 37. Wilhelmi de Toledo, F. *et al.* Fasting therapy an expert panel update of the 2002 consensus guidelines. *Forsch Komplementmed* 20, 434–443 (2013).
- 38. Bahr, L. S. *et al.* Fasting, ketogenic, and anti-inflammatory diets in multiple sclerosis: a randomized controlled trial with 18-month follow-up. *BMC Nutr* 11, 167 (2025).
- 39. Vieira-Silva, S. *et al.* Species—function relationships shape ecological properties of the human gut microbiome. *Nat Microbiol* 1, 1–8 (2016).
- 40. Volodina, E., Schürmann, M., Lindenkamp, N. & Steinbüchel, A. Characterization of propionate CoAtransferase from Ralstonia eutropha H16. *Appl Microbiol Biotechnol* 98, 3579–3589 (2014).
- 41. Paoli, A. et al. Ketogenic Diet and Microbiota: Friends or Enemies? Genes 10, 534 (2019).
- 42. Attaye, I., van Oppenraaij, S., Warmbrunn, M. V. & Nieuwdorp, M. The Role of the Gut Microbiota on the Beneficial Effects of Ketogenic Diets. *Nutrients* 14, 191 (2021).
- 43. Kitzler, H. H. *et al.* Exploring in vivo lesion myelination dynamics: Longitudinal Myelin Water Imaging in early Multiple Sclerosis. *Neuroimage Clin* 36, 103192 (2022).
- 44. Sundvall, L. *et al.* Differentiation of MS lesions through analysis of microvascular distribution. *Imaging Neuroscience* 2, imag-2-00357 (2024).
- 45. Maifeld, A. *et al.* Fasting alters the gut microbiome reducing blood pressure and body weight in metabolic syndrome patients. *Nat Commun* 12, 1970 (2021).
- 46. Sato, K., Nakashima, A., Fukuda, S., Inoue, J. & Kim, Y.-G. Fasting builds a favorable environment for effective gut microbiota modulation by microbiota-accessible carbohydrates. *BMC Microbiol* 25, 414 (2025).
- 47. Russell, W. R. *et al.* Major phenylpropanoid-derived metabolites in the human gut can arise from microbial fermentation of protein. *Molecular Nutrition & Food Research* 57, 523–535 (2013).
- 48. Rosario, D. *et al.* Understanding the Representative Gut Microbiota Dysbiosis in Metformin-Treated Type 2 Diabetes Patients Using Genome-Scale Metabolic Modeling. *Front Physiol* 9, 775 (2018).

- 49. Mohsen, E., Haffez, H., Ahmed, S., Hamed, S. & El-Mahdy, T. S. Multiple Sclerosis: A Story of the Interaction Between Gut Microbiome and Components of the Immune System. *Mol Neurobiol* 62, 7762–7775 (2025).
- 50. Ferraris, C. *et al.* One Month of Classic Therapeutic Ketogenic Diet Decreases Short Chain Fatty Acids Production in Epileptic Patients. *Frontiers in Nutrition* 8, (2021).
- 51. Güzey Akansel, M. *et al.* Effects of the Ketogenic Diet on Microbiota Composition and Short-Chain Fatty Acids in Women with Overweight/Obesity. *Nutrients* 16, 4374 (2024).
- 52. Fristedt, R., Ruppert, V., Trower, T., Cooney, J. & Landberg, R. Quantitation of circulating short-chain fatty acids in small volume blood samples from animals and humans. *Talanta* 272, 125743 (2024).
- 53. Ecklu-Mensah, G. *et al.* Gut microbiota and fecal short chain fatty acids differ with adiposity and country of origin: the METS-microbiome study. *Nat Commun* 14, 5160 (2023).
- 54. Parada Venegas, D. *et al.* Short Chain Fatty Acids (SCFAs)-Mediated Gut Epithelial and Immune Regulation and Its Relevance for Inflammatory Bowel Diseases. *Front. Immunol.* 10, (2019).
- 55. De la Cuesta-Zuluaga, J. *et al.* Higher Fecal Short-Chain Fatty Acid Levels Are Associated with Gut Microbiome Dysbiosis, Obesity, Hypertension and Cardiometabolic Disease Risk Factors. *Nutrients* 11, 51 (2019).
- 56. Paoli, A. *et al.* Common and divergent molecular mechanisms of fasting and ketogenic diets. *Trends in Endocrinology & Metabolism* 35, 125–141 (2024).
- 57. Reichard, G. A., Owen, O. E., Haff, A. C., Paul, P. & Bortz, W. M. Ketone-body production and oxidation in fasting obese humans. *J. Clin. Invest.* 53, 508–515 (1974).
- 58. Reger, M. A. *et al.* Effects of β-hydroxybutyrate on cognition in memory-impaired adults. *Neurobiology of Aging* 25, 311–314 (2004).
- 59. Dąbek, A., Wojtala, M., Pirola, L. & Balcerczyk, A. Modulation of Cellular Biochemistry, Epigenetics and Metabolomics by Ketone Bodies. Implications of the Ketogenic Diet in the Physiology of the Organism and Pathological States. *Nutrients* 12, 788 (2020).
- 60. Joshi, S., Shi, R. & Patel, J. Risks of the ketogenic diet in CKD the con part. *Clinical Kidney Journal* sfad274 (2023) doi:10.1093/ckj/sfad274.
- 61. Popiolek-Kalisz, J. Ketogenic diet and cardiovascular risk state of the art review. *Current Problems in Cardiology* 49, 102402 (2024).
- 62. Crosby, L. *et al.* Ketogenic Diets and Chronic Disease: Weighing the Benefits Against the Risks. *Front. Nutr.* 8, (2021).
- 63. Effinger, D. *et al.* A ketogenic diet substantially reshapes the human metabolome. *Clin Nutr* 42, 1202–1212 (2023).
- 64. Heischmann, S. *et al.* Regulation of kynurenine metabolism by a ketogenic diet. *J Lipid Res* 59, 958–966 (2018).
- 65. Manor, O. & Borenstein, E. Systematic characterization and analysis of the taxonomic drivers of functional shifts in the human microbiome. *Cell Host Microbe* 21, 254–267 (2017).

- 66. Sakurai, T., Odamaki, T. & Xiao, J. Production of Indole-3-Lactic Acid by Bifidobacterium Strains Isolated from Human Infants. *Microorganisms* 7, 340 (2019).
- 67. Rew, L., Harris, M. D. & Goldie, J. The ketogenic diet: its impact on human gut microbiota and potential consequent health outcomes: a systematic literature review. *Gastroenterol Hepatol Bed Bench* 15, 326–342 (2022).
- 68. Ang, Q. Y. *et al.* Ketogenic diets alter the gut microbiome resulting in decreased intestinal Th17 cells. *Cell* 181, 1263–1275.e16 (2020).
- 69. Wang, G. *et al.* Microbiota-derived indoles alleviate intestinal inflammation and modulate microbiome by microbial cross-feeding. *Microbiome* 12, 59 (2024).
- 70. Ehrlich, A. M. *et al.* Indole-3-lactic acid associated with Bifidobacterium-dominated microbiota significantly decreases inflammation in intestinal epithelial cells. *BMC Microbiol* 20, 357 (2020).
- 71. Anesi, A. *et al.* Metabolic Profiling of Human Plasma and Urine, Targeting Tryptophan, Tyrosine and Branched Chain Amino Acid Pathways. *Metabolites* 9, 261 (2019).
- 72. Holle, J. *et al.* Inflammation in Children with CKD Linked to Gut Dysbiosis and Metabolite Imbalance. *J Am Soc Nephrol* 33, 2259–2275 (2022).
- 73. García-Rivera, M. A., Fernández-Ochoa, Á., Brüning, U., Fritsche-Guenther, R. & Kirwan, J. A. Identification and validation of small molecule analytes in mouse plasma by liquid chromatographytandem mass spectrometry: A case study of misidentification of a short-chain fatty acid with a ketone body. *Talanta* 242, 123298 (2022).
- 74. Dunn, W. B. *et al.* Procedures for large-scale metabolic profiling of serum and plasma using gas chromatography and liquid chromatography coupled to mass spectrometry. *Nat Protoc* 6, 1060–1083 (2011).
- 75. Luan, H., Ji, F., Chen, Y. & Cai, Z. statTarget: A streamlined tool for signal drift correction and interpretations of quantitative mass spectrometry-based omics data. *Analytica Chimica Acta* 1036, 66–72 (2018).
- 76. Coelho, L. P. *et al.* NG-meta-profiler: fast processing of metagenomes using NGLess, a domain-specific language. *Microbiome* 7, (2019).
- 77. Ruscheweyh, H.-J. *et al.* Cultivation-independent genomes greatly expand taxonomic-profiling capabilities of mOTUs across various environments. *Microbiome* 10, 212 (2022).
- 78. Kanehisa, M., Furumichi, M., Sato, Y., Kawashima, M. & Ishiguro-Watanabe, M. KEGG for taxonomy-based analysis of pathways and genomes. *Nucleic Acids Res* 51, D587–D592 (2023).
- 79. Coelho, L. P. et al. Towards the biogeography of prokaryotic genes. Nature 601, 252-256 (2022).
- 80. Buuren, S. van & Groothuis-Oudshoorn, K. mice: Multivariate Imputation by Chained Equations in R. *Journal of Statistical Software* 45, 1–67 (2011).
- 81. Darzi, Y., Falony, G., Vieira-Silva, S. & Raes, J. Towards biome-specific analysis of meta-omics data. *ISME J* 10, 1025–1028 (2016).

- 82. Bauer, D. J. & Curran, P. J. Probing Interactions in Fixed and Multilevel Regression: Inferential and Graphical Techniques. *Multivariate Behavioral Research* 40, 373–400 (2005).
- 83. Dawson, J. F. Moderation in Management Research: What, Why, When, and How. *J Bus Psychol* 29, 1–19 (2014).
- 84. Bates, D., Mächler, M., Bolker, B. & Walker, S. Fitting Linear Mixed-Effects Models Using Ime4. Journal of Statistical Software 67, 1–48 (2015).
- 85. Searle, S. R., Speed, F. M. & Milliken, G. A. Population Marginal Means in the Linear Model: An Alternative to Least Squares Means. *The American Statistician* 34, 216–221 (1980).
- 86. Oksanen, J. *et al.* vegan: Community Ecology Package. The R Foundation https://doi.org/10.32614/cran.package.vegan (2001).
- 87. Tingley, D., Yamamoto, T., Hirose, K., Keele, L. & Imai, K. mediation: R Package for Causal Mediation Analysis. *Journal of Statistical Software* 59, 1–38 (2014).

Figures

RRMS Patients

- Stable or no DMT
- Recent disease activity
- EDSS < 4.5

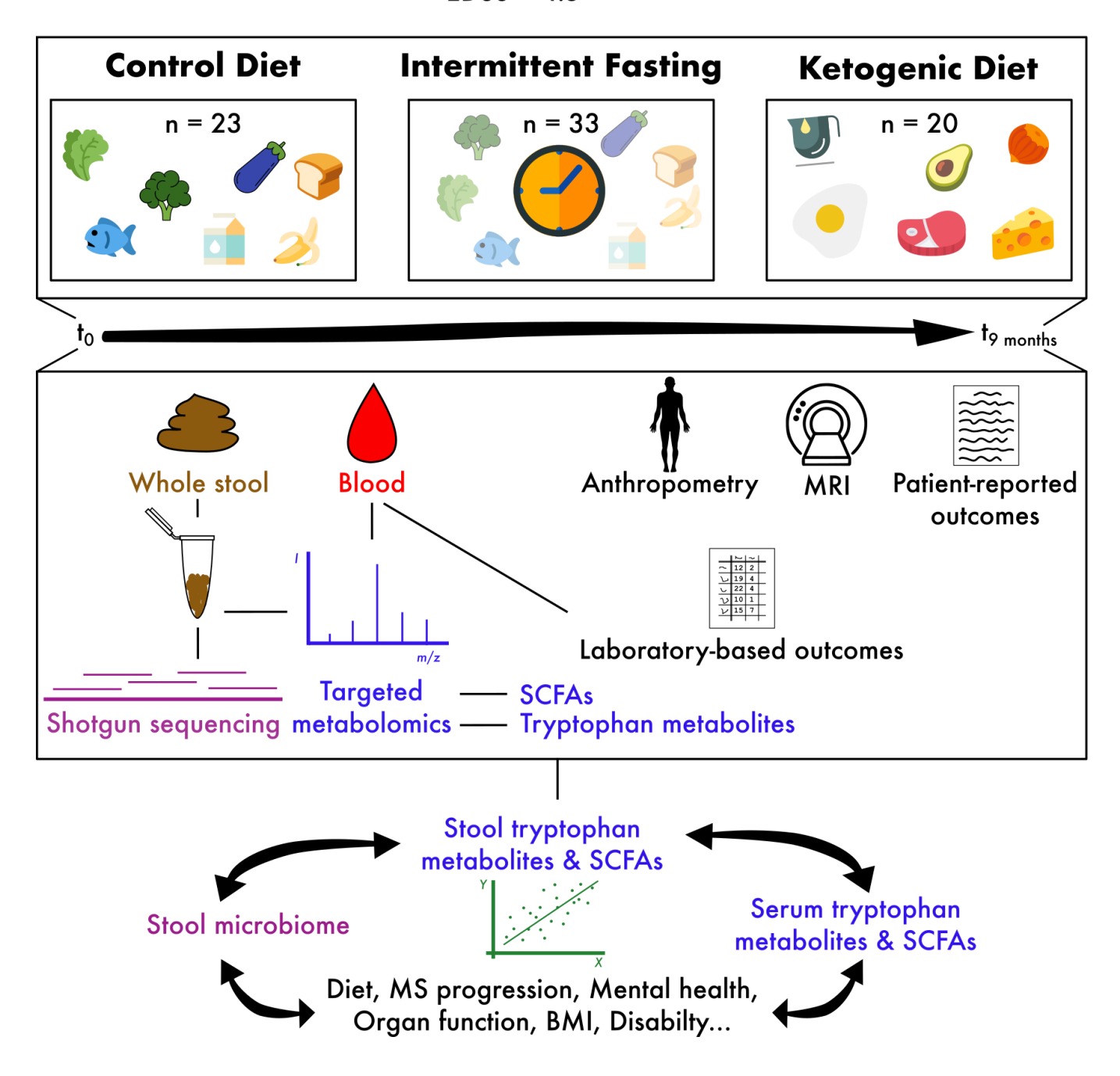


Figure 1

The NAMS cohort comprised RRMS patients with stable or no DMT treatment, recent disease activity, and an EDSS score below 4.5 [38]. Participants were randomized into three intervention groups: a healthy, predominantly vegetarian Mediterranean control diet, the same diet but with intermittent fasting plus a 7-day fast every six months, and a ketogenic diet. At baseline (t_0) and 9 months after (t_9) the start of the interventions, blood and whole stool samples were collected alongside anthropometric measures,

MRI scans, and patient-reported outcomes, including cognition, disability, and mental health assessments. Blood samples were processed for standard clinical markers such as insulin and leptin. Stool samples were homogenized, and aliquots were subjected to shotgun metagenomic sequencing. Blood serum and stool samples were analyzed for SCFA and tryptophan metabolites profiles using two distinct targeted metabolomics approaches.

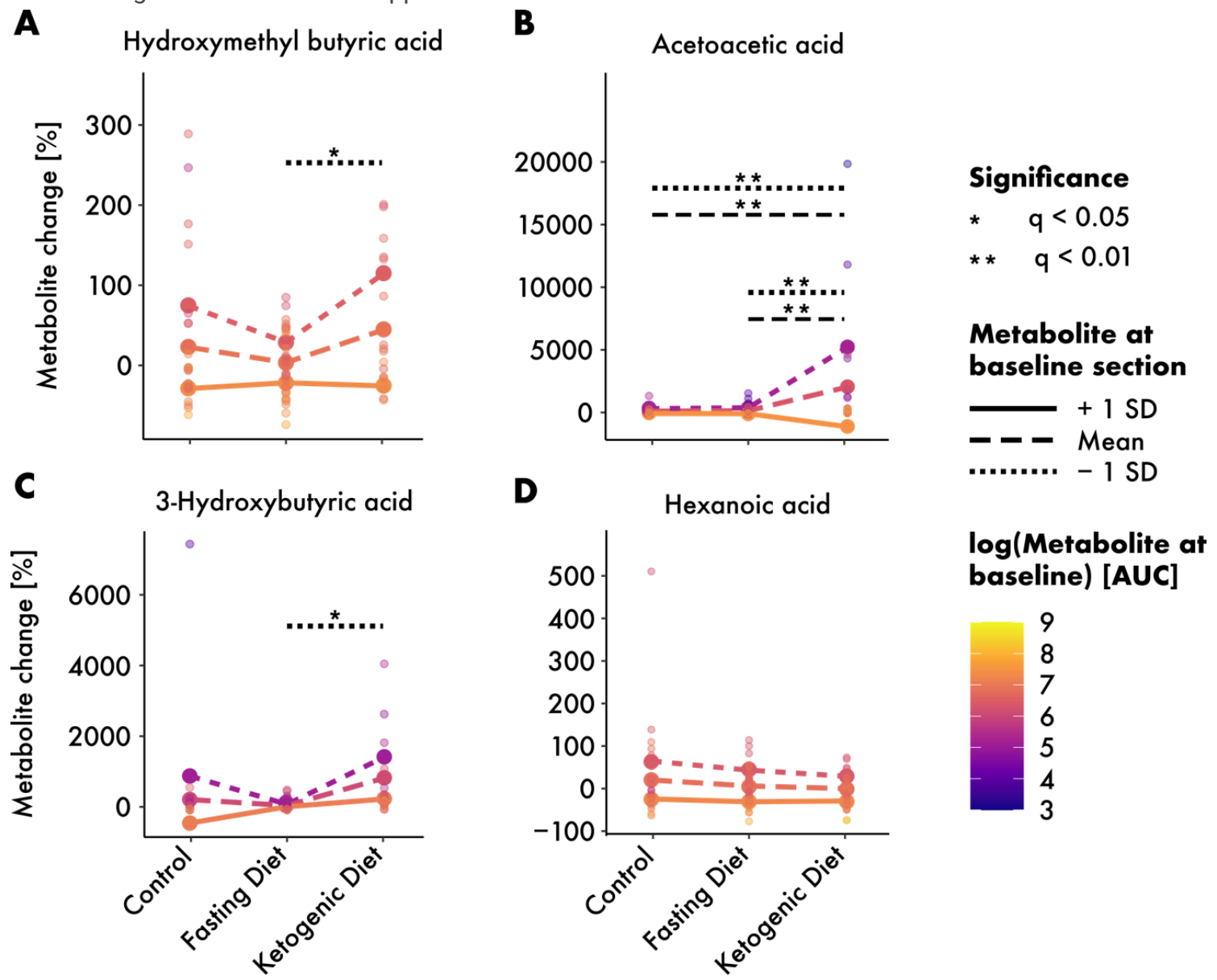


Figure 2

Changes in serum SCFAs and ketone bodies from baseline to 9-month visit, stratified by baseline SCFA values and dietary intervention. The log baseline value mean and +/- one standard deviation are highlighted per intervention and connected by differently dashed lines. Statistical significance after FDR correction is indicated by equally spaced dashed lines. (A) Patients with below-average hydroxymethyl butyric acid baseline values showed significantly greater increases in hydroxymethyl butyric acid levels under KD compared to FD. (B) Patients with average to below-average acetoacetic acid baseline values showed significantly greater increases in acetoacetic acid levels under KD compared to both FD and CD.

(C) Patients with below-average 3-hydroxybutyric acid baseline values showed significantly greater increases in 3-hydroxybutyric acid levels under KD compared to FD. (D) No significant differences between dietary interventions were observed for hexanoic acid levels.

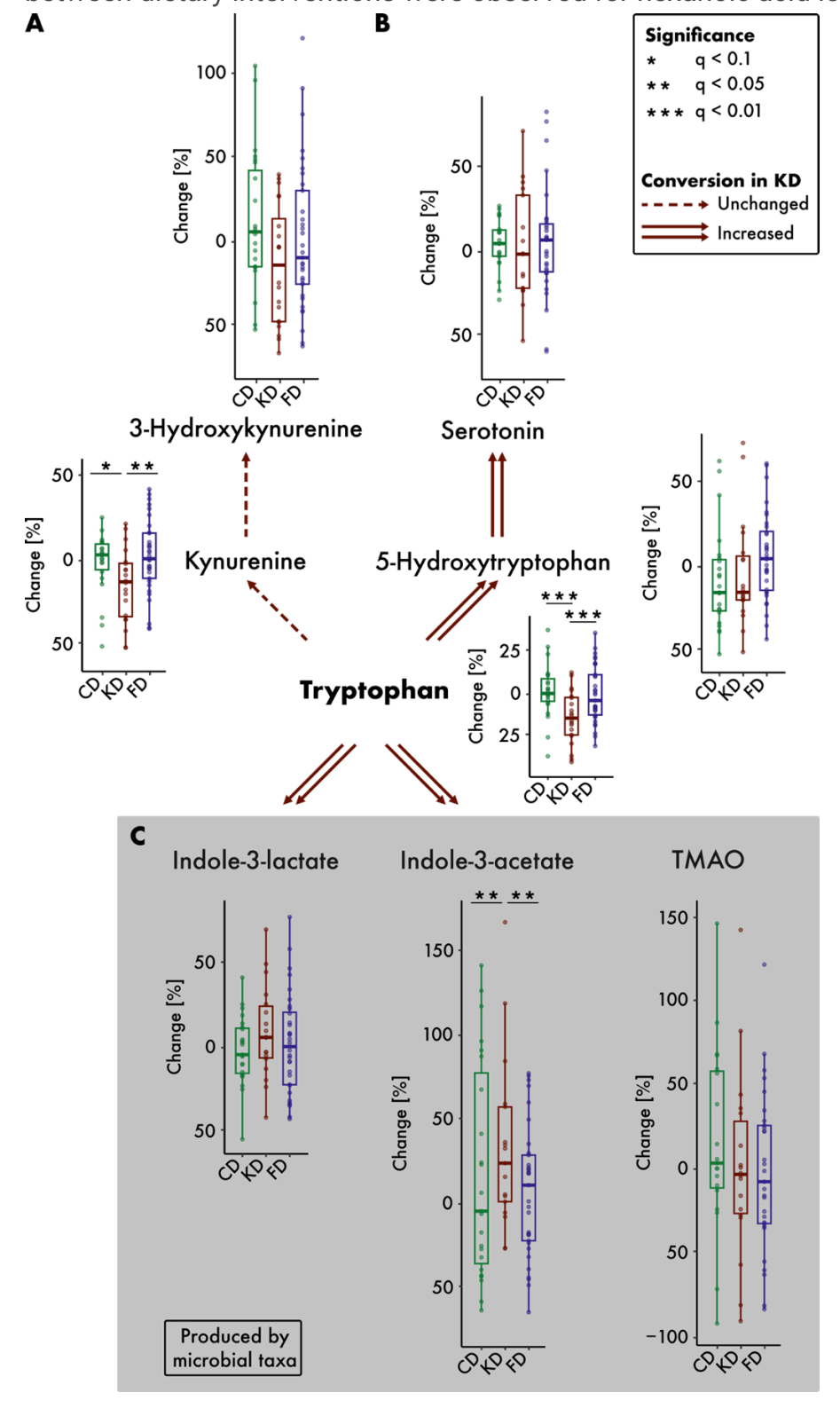


Figure 3

AUC changes per patient and group for tryptophan metabolites demonstrating metabolism shifts in response to KD. Outliers were removed for visualization only. Significance was determined post hoc

using estimated marginal means. (**A**) Kynurenine pathway metabolites followed the pattern observed for tryptophan. (**B**) Serotonin pathway metabolites were not decreased under KD despite decreased tryptophan levels. (**C**) Gut microbiome-produced indole derivatives and TMAO were not decreased under KD despite decreased tryptophan levels, with indole-3-acetate showing a significant increase.

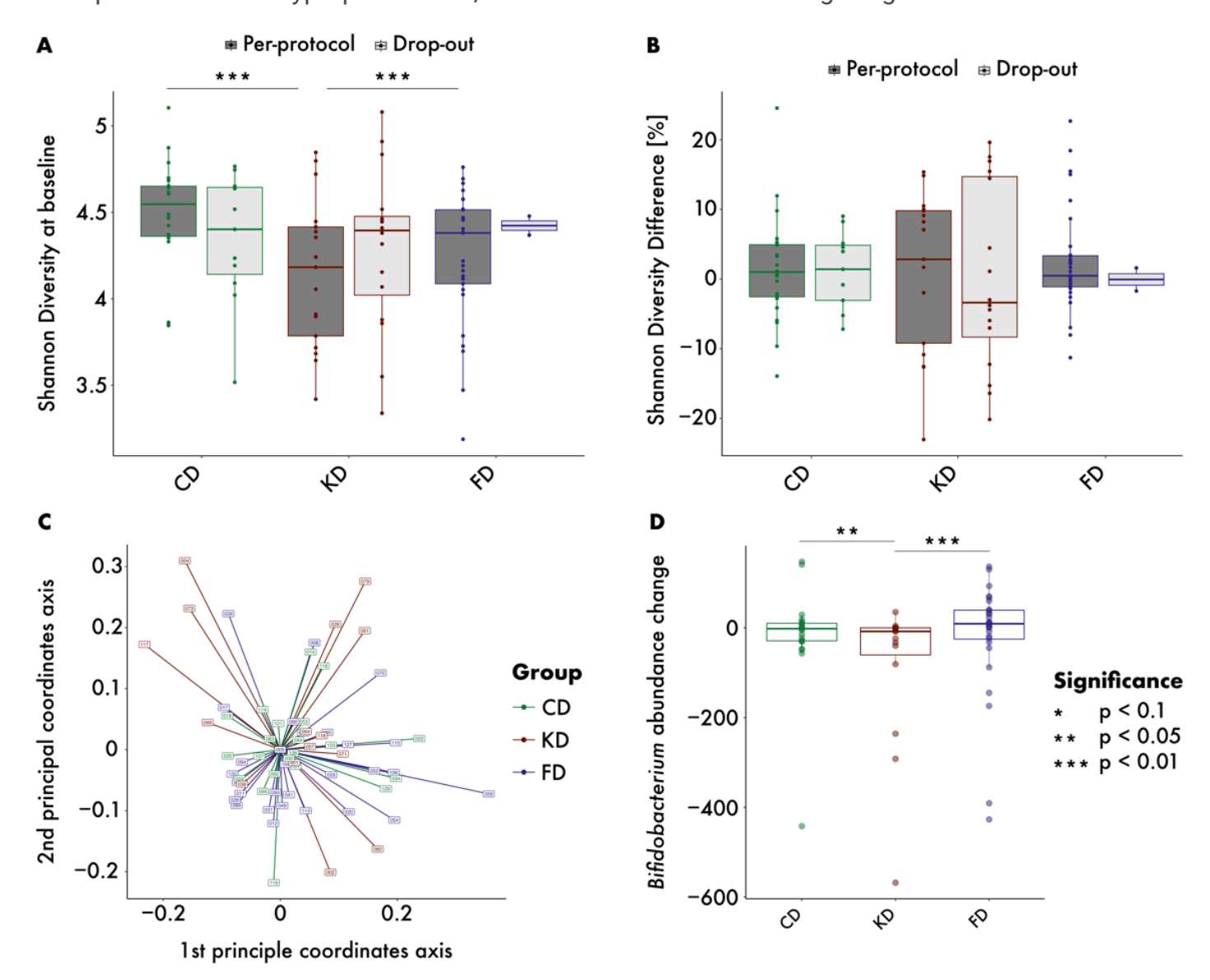


Figure 4

Microbiome shifts in response to dietary interventions. (**A**) The KD per-protocol population had a significantly lower Shannon diversity at baseline than both FD and CD groups. Significance was assessed using Dunn's test. (**B**) No significant difference in Shannon diversity changes from baseline to 9 months was observed across dietary interventions in per-protocol and dropout patients (p = 0.4). Alpha diversity values for dropout patients were imputed. (**C**) No significant beta diversity shift was detected in any diet group. (**D**) *Bifidobacterium* abundance significantly decreased in the KD group, with significance assessed using estimated marginal means.

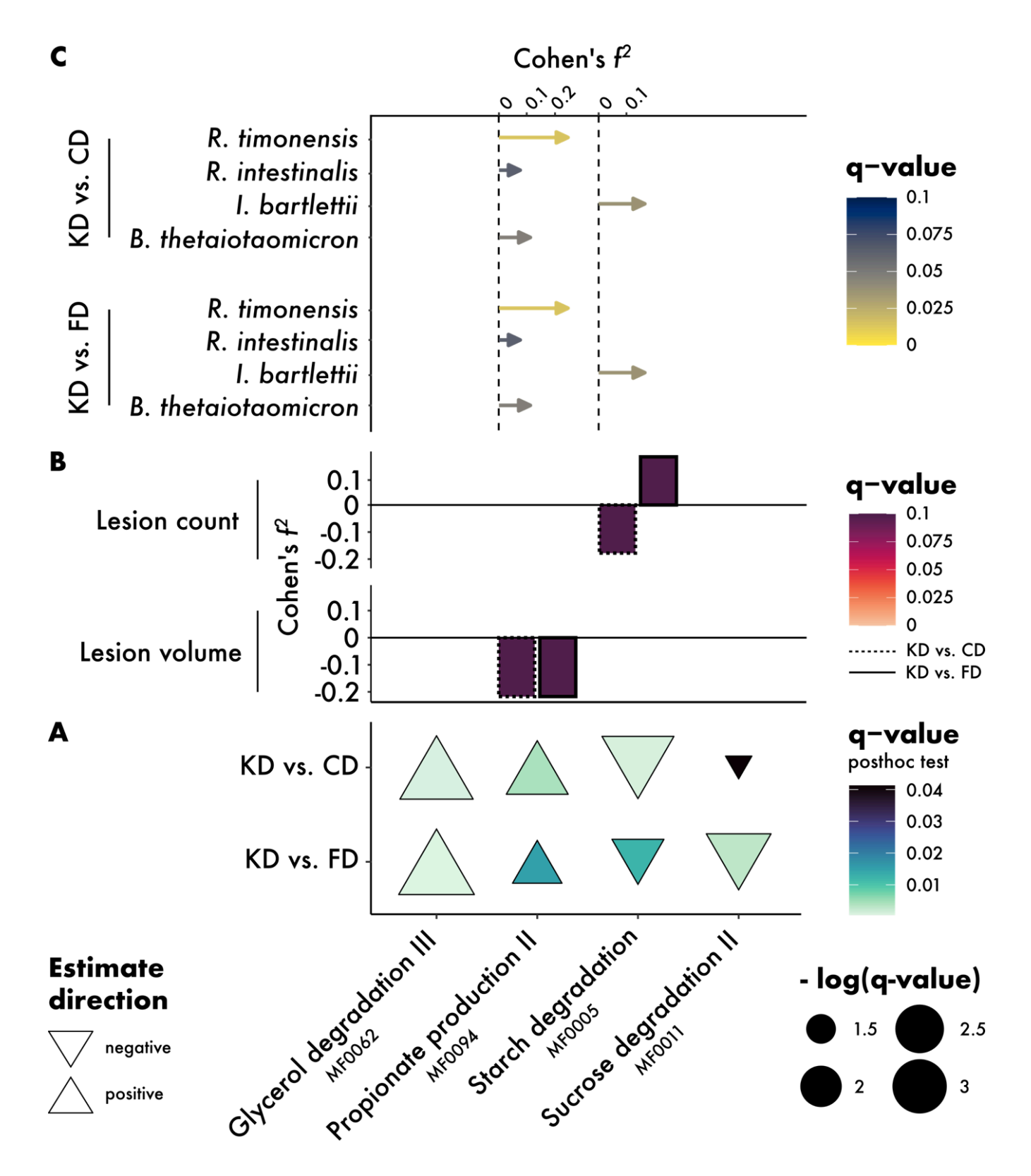


Figure 5

Gut microbial modules (GMM) link diet to lesion outcomes. (A) Post hoc analysis revealed that two GMMs increased and two decreased significantly more under KD compared to the other two diets. (B) The association between propionate production II (MF0094) and lesion volume became more negative under KD compared to the other two diets. The association between starch degradation (MF0005) and lesion count became more strongly negative in KD versus CD and more strongly positive in KD versus FD.

(C) Four species that mirrored the GMM-outcome relationship showed stronger positive associations with propionate production II (MF0094) and starch degradation (MF0005) under KD compared to the other two diets.

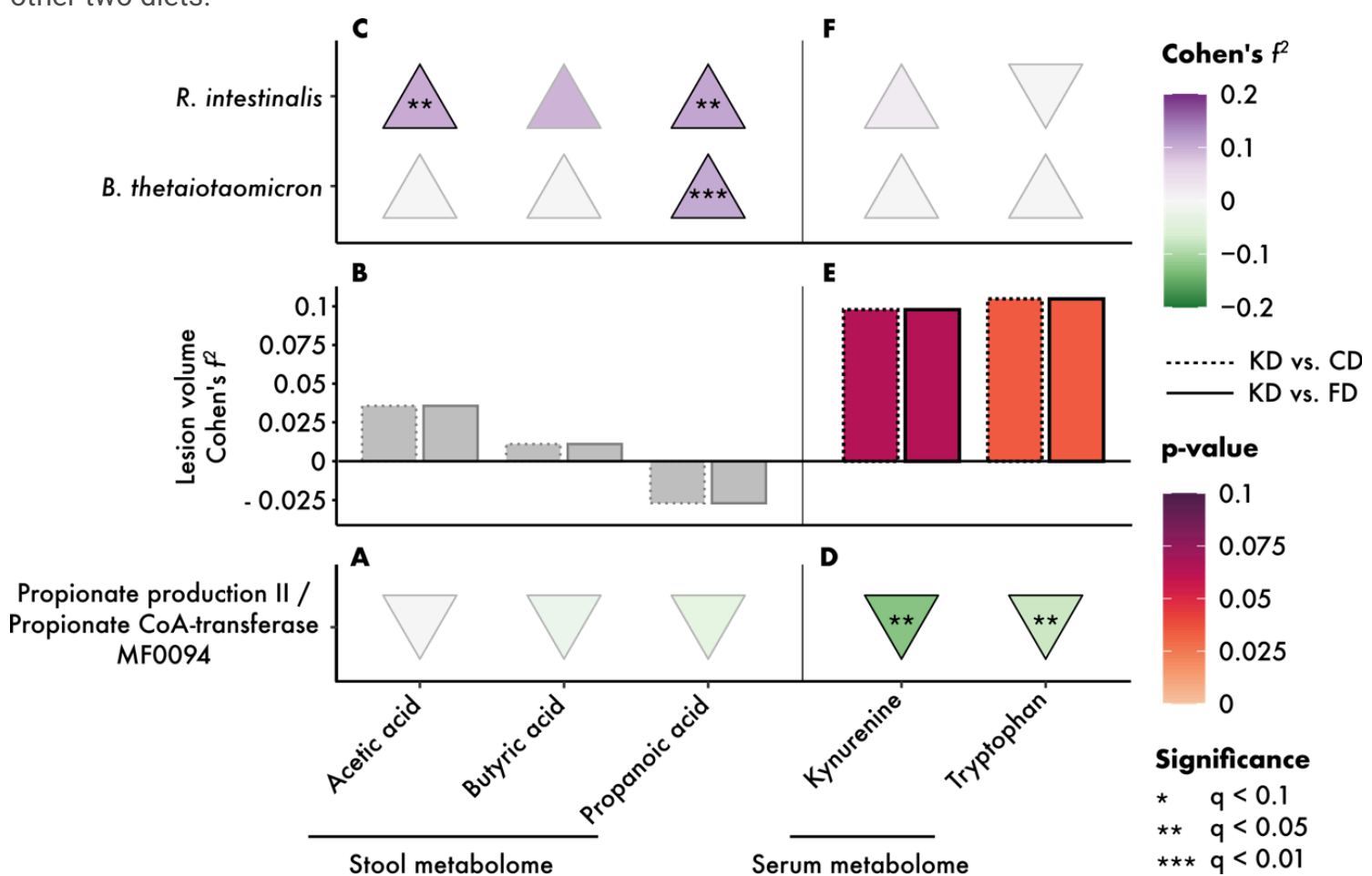


Figure 6

Metabolome-microbiome associations with MS outcomes. (A) Stool metabolites showed no association with propionate production II (MF0094). (B) Stool metabolites demonstrated no significant relationship with lesion volume over time ($q_{Acetic\ acid,\ Propanoic\ acid} = 0.6$, $q_{Butyric\ acid} = 0.71$). (C) Two lesion volume-related species showed correlations with two stool SCFAs across groups. (D) Two group-associated serum metabolites, tryptophan and kynurenine, were negatively associated with propionate production II (MF0094). (E) Serum tryptophan and kynurenine exhibited a significantly more positive association with lesion volume in KD compared to FD and CD. (F) No association was observed between serum tryptophan and kynurenine and either propionate production II (MF0094) or lesion volume-related species.

Supplementary Files

This is a list of supplementary files associated with this preprint. Click to download.

SupplementsNAMSMicrobiomeMetabolome.docx